

Au₂₅ Gold Nanoclusters for Enhancing Organic Cell Parameters

Yashaswini Gowda N.
Dayananda Sagar Academy of
Technology & Management

R. V. Manjunath
Dayananda Sagar Academy of
Technology & Management

B. R. Lakshmikantha
Dayananda Sagar Academy of
Technology & Management

ABSTRACT

Ultra small gold nanoparticles (GNPs) also called gold nano clusters (GNCs) because of their unique structure comprises of very few atoms and are capable of molecular level interactions by virtue of their molecule like properties. Introduction of GNCs to assist the transport layer of organic solar cells fetched higher current output as compared to cells with GNPs and cells with no gold at all. GNC devices showed a maximum efficiency enhancement by a factor of 1.74 to that of reference cell without gold. Faster electron-hole separation and movement towards respective electrodes leads to better efficiency and we suggest that electronic properties of GNCs enhance the action of transport layer PEDOT:PSS. But GNCs give more to the solar cell. They also allow more light to pass through them, thus, allowing more light to reach the active layer via transport layer, leading to increase in photocurrent resulting in overall parameter enhancement. It was evident with our experiments that single layer of GNCs provides double benefits of transport enhancement and absorption enhancement adding up to increased cell parameters and efficiency keeping the low cost advantage of organic solar cells intact.

Keywords

Nanoclusters, Gold Nanoparticles, Organic Cells, Current Density

1. INTRODUCTION

Polymeric organic solar cells (PSCs) are being researched upon extensively due to their many advantages over inorganic solar cells primarily being their high portability, low manufacturing cost, mechanical and chemical flexibility and their light weight. However, parameters such as insufficient light absorption and low carrier mobilities make them inferior to the inorganic solar cells and are hindering PSCs commercialization. Spectral mismatch between the absorption spectrum and solar spectrum and inefficient charge separation and transport also account for reduced cell performance of organic photovoltaic devices [1]. Researchers worldwide have been trying different ways to overcome these parameters in order to achieve high current output, thus, obtaining enhanced cell parameters such as current density (J_{sc}), open-circuit voltage (V_{oc}), fill factor (FF) and overall cell efficiency (η).

Incorporating noble metal nanoparticles into the different polymer layers has been identified as a way of enhancing cell parameters [1][2][3][4][5][6]. Introducing gold and silver metal nanoparticles into active layer enhances the layer's absorptivity leading to more exciton generating electrons on the surface of electrode resulting in increased current. The increase in absorptivity is independent of nanoparticle size rather proportional to its volume fraction[7]. Doping the transport layer with nanoparticles leads to faster electron-hole transportation towards respective electrodes resulting in increased efficiency[2]. To further improve efficiency, doping

of both active layer and transport layer was done simultaneously in a device[3]. Increasing the volume of gold, although increases efficiency but it also increases the cost of device fabrication thereby defeating the low cost advantage of organic solar cells over silicon based cells.

Recently, few scientists tried ultra small gold nanoparticles also categorized as gold nanoclusters owing to their unique optical and electrical properties and achieved enhancement in solar cell efficiency and reducing the amount of gold used otherwise by a huge margin keeping the low-cost advantage of organic cells intact.

GNCs are categorized differently from gold nanoparticles primarily due to difference in their structures and uniqueness in optical and electrical properties. GNCs were recognized more than a decade ago for their unique optical properties such as photoluminescence, capabilities of molecular level interaction and for their solubility and non-toxicity as well [9][10]. Taking advantage of which GNCs have been explored in numerous biomedical experiments and research [11]. Only recently, they have been explored in the field of solar harvesting [8][8a]. In late 2014, Bauld et al utilized ultra small gold nanoparticles also categorized as gold nanoclusters were layered along with PEDOT:PSS to fabricate their organic solar cell device [8]. They achieved an enhancement by a factor of 0.9 as compared to reference cells. Enhancement factor is given by ratio of efficiency of device in focus to the efficiency of reference device. Earlier this year, Kamat et al used GNCs as a photosensitizer along with sensitizing squaraine dye in their organic dye sensitized solar cells [8a]. Replacing squaraine dye with GNCs as photosensitizer did not show much improvement but using both the material simultaneously leads to increase in efficiency by a factor of 2.

GNCs consisting of merely tens to hundreds of gold atoms are sized less than 1 to 3 nm in diameter [12]. Their ultra small size corresponds to the Fermi wavelength of electron leading to quantum confinement of free electrons and resulting in the formation of discrete electronic states in the compact nanoclusters [13][14]. Also, the capability of controlling the number of atoms in these clusters makes them a material of great interest. To observe and explore more properties dependent on the number of atoms in the GNCs can help shed more light on it's working role and mechanism.

Various protecting ligands ranging from small molecules like glutathione to large molecular weight proteins such as bovine serum albumin (BSA) have been used to synthesize gold nanoclusters in a bottom-up using a gold precursor and reducing agents along with protecting ligands (glutathione and BSA). Number of atoms ranging from as low as 12 to as high as 300 has been achieved using these approaches [16]. BSA protected GNCs are easy to prepare under ambient conditions and reaction times can be varied in proportion with temperature. They also exhibit higher quantum yield and better photostability than glutathione protected GNCs

[17][18][19]. Gold nanoclusters can also be prepared by top down approaches such as ligand inducing etching but compromising with the ease of synthesis.

Works reported above [8][8a] utilizes glutathione protected GNCs consisting of 144 gold atoms prepared by bottom-up approach. In the current work, we fabricated polymer based organic solar cell devices utilizing BSA protected gold nanoclusters (GNCs) to assist transport layer in device efficiency enhancement. To compare its performance, devices with a layer of gold nanoparticles (GNPs) and a reference device without any gold nanostructure were also fabricated. BSA protected GNCs used in our work consists of 25 atoms (Au₂₅) [20] which is considerably less than 144 atoms glutathione protected GNCs (Au₁₄₄). The photophysical properties of these nanoclusters are strongly correlated to their size,[27-31] ligand,[32][33] and composition [34-37]. It has been shown in one case that catalytic properties are dependent of number of atoms in the gold nanoclusters [15]. Au₂₅ is a 25 atom cluster with BSA as protecting ligand and icosahedral structure. We experiment to see effects of changing the number of atoms and type of ligand on the device performance parameters.

2. Materials and Methods

2.1 Materials

Gold precursor i.e. chloroauric acid (HAuCl₄) was common for GNC and GNP synthesis. Bovine serum albumins (BSA), sodium hydroxide (NaOH) were required for GNC preparation. Trisodium citrate for GNP synthesis. Poly-3,4-ethylene-dioxythiophene:poly-styrene-sulfonate (PEDOT:PSS), Poly(3-Hexyl-Thiophene-2,5-diyl) (P3HT), [6,6]-Phenyl-C61-Butyric acid Methyl ester (PCBM), aluminum beads were required for device fabrication. All the material were purchased from Sigma Aldrich, USA and used without further purification. ITO-glass was purchased from local vendor.

2.2 Methods

Synthesis of GNCs was carried out by using protocol reported by Ying et al [21]. Briefly, 5 mL HAuCl₄ (10 mM) was mixed with 5 mL aqueous solution of BSA (50 mg/mL). The reaction was kept on vigorous stirring and NaOH was added two minutes after stirring has started. The mixture was left to stir for 12 hours at room temperature (37^o C). The yellow color of the mixture changes to light brown and eventually to deep brown confirming the successful synthesis of BSA protected GNCs.

GNPs were synthesized using well known citrate reduced method [22].

Polymeric solar cell was fabricated by using layer by layer deposition on an indium-tin oxide (ITO) glass substrate in a clean environment. ITO substrates in the multiples of three were cleaned under ultrasonication. Firstly by soap water, followed by acetone, followed by isopropanol and were blow dried. Further the substrates were subjected to plasmon heating for 10 minutes to improve the work function of ITO. Samples were then marked 1, 2 and 3; 4, 5 and 6 and so on. Six such sets were made. To samples 1, 4, 7, etc, AuNCs were spin coated at 8000 rpm and annealed at 400^oC for 9 minutes to remove excess BSA and to give rise to a uniform tessellated structure of GNCs [8]. To samples 2, 5, 8, etc, AuNPs were spin coated at 8000 rpm and annealed at 400^oC for 9 minutes. Rest other samples were not coated with plasmon enhancing gold layer and were used as reference cells. Transport layer of PEDOT:PSS was then coated on all

the samples at 4000 rpm and annealed at 140^oC to remove excess water. Active layer of heterogeneous mixture of P3HT:PCBM was spin coated at 2000 rpm and heated at 60^oC for 5 minutes to increase charge mobility of the material as it is then kept to cool down. Aluminum electrodes were then patterned on all the substrates using physical vapor deposition. After successful completion of last step, all prepared samples were kept on hot plate for post production treatment by heating at 140^oC for 4 minutes and removed once the temperature came down to 60^oC.

We thus fabricated six sets of three different types of devices, one type of device with AuNCs layer, one with AuNPs layer and a reference device containing no gold layer.

3. CHARACTERIZATION

Transmission electron images are recorded using Tecnai G2 F30 S-Twin (FEI; Super twin lens with Cs=1.2 mm) instrument operated at accelerating voltage at 300 KV, having a point resolution of 0.2 nm and Lattice resolution of 0.14 nm). Scanning electron microscopy was done using Zeiss EVO MA 10 at 5kV beam voltage. UV-Vis measurements were done using Agilent Technologies Cary 500 UV-Vis-NIR spectrometer. Current Voltage analysis was done using a tungsten lamp and data was analyzed using Agilent I-V measurement software. Surface morphology study was done using atomic force microscopy.

4. RESULTS AND DISCUSSION

Fig. 1 shows transmission electron microscopy images of as prepared BSA protected GNCs with sizes less than 1 nm to 5 nm.

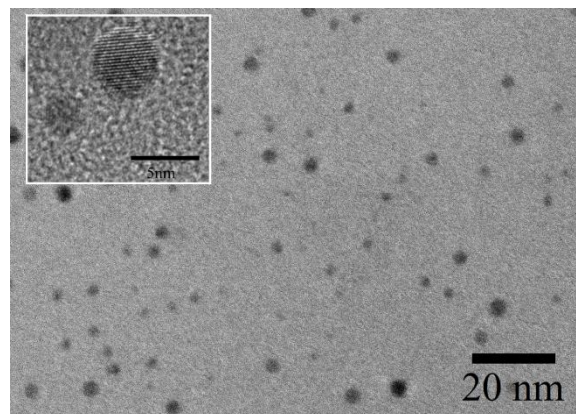


Fig. 1. TEM images of BSA protected gold nanoclusters (size 1-5 nm) Scale : 20 nm. Inset scale : 5 nm

ITO-PEDOT:PSS interface is not stable due to the strong acidic nature of PEDOT:PSS which leads to the corrosion of ITO and indium diffusion into PEDOT:PSS and polymer layer resulting in variation in surface morphology and higher roughness [23][24][25][26] which no longer remains a reason once GNCs are introduced as ITO and PEDOT:PSS are no longer in direct contact.

SEM characterization (fig. 3) of different films gave as expected results. Fig. 3 a-b shows GNPs on the ITO layer with size ranging from 40-50nm. There was little effect of annealing on GNPs layers. Fig 3. c-d shows a different scenario altogether. In Fig. 3 c. we see a BSA bed on top of our glass/ITO surface in which GNCs are embedded but not visible. After annealing this layer at 400^oC, fig 3 d. revealed

row wise assembly of colonies of GNCs as the BSA was evaporated.

As evident from the SEM image, GNCs are uniformly colonized all over the ITO film.

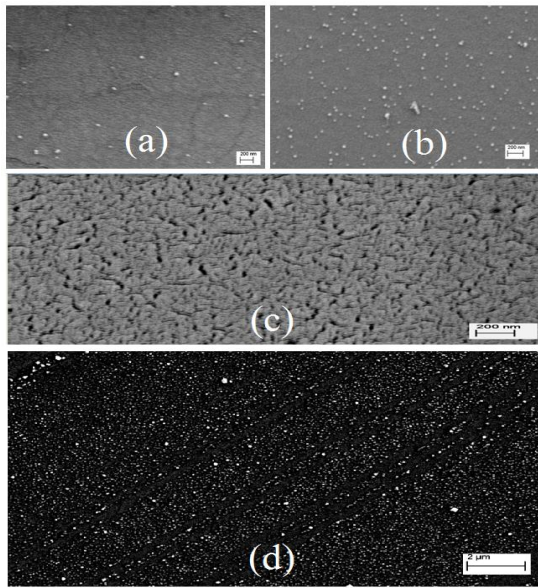


Fig 3. a) AuNPs on ITO (scale bar : 200 nm) b) AuNPs annealed at 400°C (scale bar : 200 nm) c) BSA-AuNCs on ITO (scale bar : 200 nm) d) AuNCs annealed at 400°C (scale bar : 2 μm)

Table 1a shows I-V measurements of first devices fabricated with GNC layer and without GNCs as reference cell. We observed increment in J_{sc} , V_{oc} and FF of devices containing GNCs as compared to reference cell. (Efficiency could not be measured directly for any device due to lack of instrument specification i.e. input power intensity.)

Table 1b shows performance enhancement factors for all the parameters compared between device with GNCs and reference cell. Efficiency enhancement factor was calculated mathematically.

Cell Parameters	With GNC	Reference Cell
J_{sc} (mA/mm ²)	2.91	2.01
V_{oc} (V)	0.593	0.576
FF (%)	38.4	34.6

(a)

Performance Factors	GNC/Reference	Percentage Increase
J_{sc}	1.45	45%
V_{oc}	1.03	3%
FF	1.11	11%
Efficiency	1.65	65%

(b)

Table 1 : a) Measured cell parameters of devices with and without (reference) GNCs b) Performance enhancement factors of devices with GNCs over devices without GNCs. Performance enhancement factor for efficiency was deduced mathematically.

Efficiency for a device is given by,

$$\eta = P_{out} / P_{in} \quad (1)$$

P_{out} and P_{in} being the output and input power respectively.

$$P_{out} = V_{oc} \times J_{sc} \times FF \quad (2)$$

Equating eq. 2 in eq. 1 we get,

$$\eta = V_{oc} \times J_{sc} \times FF / P_{in} \quad (3)$$

$$\eta_{GNC} = V_{oc1} \times J_{sc1} \times FF1 / P_{in1}$$

$$\eta_{ref} = V_{oc2} \times J_{sc2} \times FF2 / P_{in2}$$

Parameter enhancement factor (p.e.f.) is given by,

p.e.f. = Parameter Value of device in focus / Parameter value of reference device...(4)

Therefore, efficiency enhancement factor (e.e.f.) is given by,

$$e.e.f. = \eta_{GNC} / \eta_{ref} = \frac{V_{oc1} \times J_{sc1} \times FF1}{P_{in1}} \times \frac{P_{in2}}{V_{oc2} \times J_{sc2} \times FF2} \quad (5)$$

But $P_{in1} = P_{in2}$ as both devices were measured under same source (tungsten lamp)

Putting values from table 1a into equation 5 we get

$$e.e.f. = 1.65$$

Our results indicate a 65% increase in the efficiency of device with GNCs layer as compared to the reference cell without it.

Repeated fabrication and measurements showed a consistent enhancement in parameters of devices with GNCs over reference devices reaching a maximum e.e.f. of 1.74. Devices with GNP layer in between ITO and PEDOT:PSS showed even reduced cell parameters as compared to reference cell due to localized surface plasmon resonance. As GNPs were not mixed with PEDOT:PSS so they could not form a close contact with the active layer which is important as the extension of LSPR field is only few nanometers [...]. When the GNPs are placed below PEDOT:PSS layer the LSPR field decays significantly before reaching active layer, thus, having a deteriorating effect on the device parameters [8]. This field is absent in GNCs, hence placing the GNCs below PEDOT:PSS layer does not affect the GNCs role in performance enhancement.

To start investigating into the role of GNCs in this enhancement our primary target was to check the amount of light reaching active layer P3HT:PCBM after passing through ITO, GNC and PEDOT:PSS as number of electrons generated from active layer material and reaching the electrode surface are proportional to amount of light falling on the active layer. Fig. 2 shows UV-visible spectroscopy of plain ITO, ITO with PEDOT:PSS coating as used in reference cell and ITO-PEDOT:PSS with GNC layer in between them to assist the transport layer. GNC was annealed at 400°C for 9 minutes to remove BSA. PEDOT:PSS layer was also annealed for 30 minutes at 140 °C. As seen from the figure 89% of incident light on the transparent electrode ITO of the device is transmitted out of the ITO-PEDOT:PSS layers. When GNC layer is introduced between ITO and PEDOT:PSS, transmission of light now increases by ~8% transmitting 95.4% of light to the active layer.

Transmission of more light to active layer after introduction of GNC layer in between transparent electrode and the transport layer generates more number of electron hole pair from the material as compared to reference cell. This highlights the optical properties of GNCs and more insight can be drawn with further experiments.

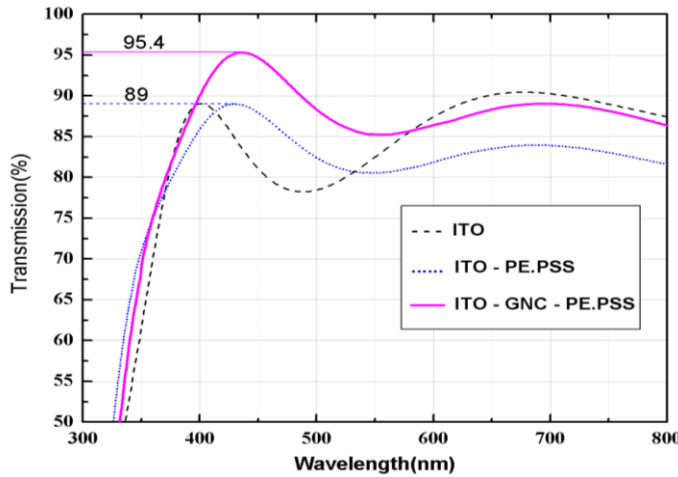


Fig. 2. UV-Vis measurement of plain ITO, ITO-PEDOTPSS, ITO-GNC-PEDOTPSS. 8% increase in transmission when AuNCs are introduced between ITO and PEDOTPSS

Advanced optical property of GNCs can now be said to have a positive effect on the parameter enhancement of the device by letting more light to pass through it to the active layer.

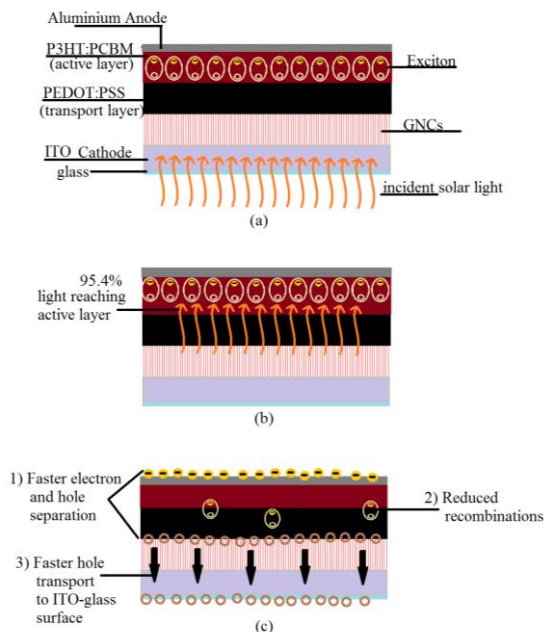


Fig. 3. a) Organic solar cell with GNC layer to assist transport layer. b) 95.4% of incident light reaches the active layer resulting in more excitons to generate electrons towards anode c) GNCs help in faster separation of electron-hole and transport towards respective electrodes as compared to reference cells. Recombination also reduces as most of the hole are transported towards the cathode with the help of GNCs.

Each GNC, as discussed earlier, consist of discrete energy levels. Their structure is a core-shell type. Au (0) atoms form the core and Au(1) atoms along with sulphur (S) atoms form the shell of these nanoclusters. Au (1) means a positive charge of +1 or an electron deficiency. This deficiency creates room for one hole to be transported across the transport layer and towards the ITO cathode much faster than it happens in the bulk as depicted in fig. 4.

5. CONCLUSION

Electrical and optical properties of advanced material Gold Nanoclusters help in the parameters enhancement of organic solar cells. Previous work uses 144 gold atoms to reach an efficiency enhancement by 10% of cells with GNCs as compared to reference cells. In our work, we use GNCs, each comprising of 25 gold atoms. Reduction in the number of gold atoms gave us an efficiency enhancement by more than 60% with maximum going upto 74% or by a factor of 1.74. GNCs improves the device parameters by a good percentage, GNCs also keep the low cost advantage of polymeric solar cells intact as amount of gold used in a single of GNCs is extremely low and bulk manufacturing would not add much to the organic cell cost. Future work can be done by utilizing GNCs of different atoms and see its effect on the cell parameters. We hope our work will open new horizons for the commercialization of organic solar cells.

6. REFERENCES

- [1] Roles of Au and Ag nanoparticles in efficiency enhancement of poly(3-octylthiophene)/C60 bulk heterojunction photovoltaic devices Kyungkon Kim1 and David L. Carroll1,a) Appl. Phys. Lett. 87, 203113 (2005); <http://dx.doi.org/10.1063/1.2128062>
- [2] Plasmonic-enhanced polymer photovoltaic devices incorporating solution-processable metal nanoparticles Fang-Chung Chen1,2,a), Jyh-Lih Wu1,3, Chia-Ling Lee1,2, Yi Hong1,2, Chun-Hong Kuo4 and Michael H. Huang4 Appl. Phys. Lett. 95, 013305 (2009)
- [3] Improving the efficiency of polymer solar cells by incorporating gold nanoparticles into all polymer layers Feng-Xian Xie1, Wallace C. H. Choy1,a), Charlie C. D. Wang1, Wei E. I. Sha1 and Dixon D. S. Fung1 Appl. Phys. Lett. 99, 153304 (2011)
- [4] APL 2006 89 093103
- [5] APL 2009 95 013305
- [6] Nat. Mater. 2010, 9, 205-13
- [7] Size dependence of spherical metal nanoparticles on absorption enhancements of plasmonic organic solar cells Inho Kim a,*, Kyu-Sung Lee b, Taek-Sung Lee a, Doo Seok Jung a, Wook-Seong Lee a, Won Mok Kim a, Kyeong-Seok Lee a Synthetic metals 199, 2015, 174-178
- [8] Tesselated paper 8a) Boosting the Photovoltage of Dye-Sensitized Solar Cells with Thiolated Gold Nanoclusters Hyunbong Choi , Yong-Siou Chen , Kevin G. Stamplecoskie , and Prashant V. Kamat *J. Phys. Chem. Lett., 2015, 6 (1), pp 217–223
- [9] Size Dependence of Atomically Precise Gold Nanoclusters in Chemoselective Hydrogenation and Active Site Structure Gao Li †, De-en Jiang ‡, Santosh

- Kumar †, Yuxiang Chen †, and Rongchao Jin *† ACS Catal., 2014, 4 (8), pp 2463–2469
- [10] Interaction of gold nanoclusters with IR light emitting cyanine dyes: a systematic fluorescence quenching study Chiranjib Banerjee, Jagannath Kuchlyan, Debasis Banik, Niloy Kundu, Arpita Roy, Surajit Ghosh and Nilmoni Sarkar* DOI: 10.1039/c4cp02563f
- [11] Fluorescent Gold Nanoclusters: Recent Advances in Sensing and Imaging Li-Yi Chen, Chia-Wei Wang, Zhiqin Yuan, and Huan-Tsung Chang* Anal. Chem. 2015, 87, 216-229
- [12] Zheng, J.; Nicovich, P. R.; Dickson, R. M. Annu. Rev. Phys.Chem. 2007, 58, 409-431.
- [13] Chen, S.; Ingram, R. S.; Hostetler, M. J.; Pietron, J. J.; Murray, R. W.; Schaaff, T. G.; Khoury, J. T.; Alvarez, M. M.; Whetten, R. L. Science 1998, 280, 2098-2101.
- [14] Lee, D.; Donkers, R. L.; Wang, G.; Harper, A. S.; Murray, R. W. J. Am. Chem. Soc. 2004, 126, 6193-6199.
- [15] Size Dependence of Atomically Precise Gold Nanoclusters in Chemoselective Hydrogenation and Active Site Structure Gao Li †, De-en Jiang ‡, Santosh Kumar †, Yuxiang Chen †, and Rongchao Jin *† ACS Catal., 2014, 4 (8), pp 2463–2469
- [16] S. Malola, L. Lehtovaara, J. Enkovaara, H. Häkkinen, "Birth of the localized surface plasmon resonance in monolayer-protected gold nanoclusters", ACS Nano 7, 10263 (2013).
- [17] Hofmann, C. M.; Essner, J. B.; Baker, G. A.; Baker, S. N. Nanoscale 2014, 6, 5425-5431.
- [18] Chen, P.-C.; Chiang, C.-K.; Chang, H.-T. J. Nanopart. Res. 2013, 15, 1-10.
- [19] Yue, Y.; Liu, T.-Y.; Li, H.-W.; Liu, Z.; Wu, Y. Nanoscale 2012, 4, 2251-2254.
- [20] Protein-directed synthesis of highly fluorescent gold nanoclusters Jianping Xie, Yuangang Zheng and Jackie Y. Ying JACS 2009 131 888-89
- [21] Xie K JACS 2009 131 (3) 888
- [22] turkevich et al
- [23] M.P. de Jong, L.J. van Ijzendoorn, M.J.A. de Voigt, Stability of the interface between indium-tin-oxide and poly(3,4-ethylenedioxythiophene)/poly(styrenesulfonate) in polymer light-emitting diodes, Appl. Phys. Lett. 77 (2000) 2255–2257.
- [24] K.W. Wong, H.L. Yip, Y. Luo, K.Y. Wong, W.M. Lau, K.H. Low, H.F. Chow, Z.Q. Gao, W.L. Yeung, C.C. Chang, Blocking reactions between indium-tin oxide and poly (3,4-ethylene dioxythiophene):poly(styrene sulphonate) with a self-assembly monolayer, Appl. Phys. Lett. 80 (2002) 2788–2790.
- [25] H. Yan, P. Lee, N.R. Armstrong, A. Graham, G.A. Evmenenko, P. Dutta, T.J. Marks, High-performance hole-transport layers for polymer light-emitting diodes. Implementation of organosiloxane cross-linking chemistry in polymeric electroluminescent devices, J. Am. Chem. Soc. 127 (2005) 3172–3183.
- [26] J. Ni, H. Yan, A. Wang, Y. Yang, C.L. Stern, A.W. Metz, S. Jin, L. Wang, T.J. Marks, J.R. Ireland, C.R. Kannewurf, MOCVD-Derived highly transparent, conductive zinc- and tin-doped indium oxide thin films: precursor synthesis, metastable phase film growth and characterization, and application as anodes in polymer light-emitting diodes, J. Am. Chem. Soc. 127 (2005) 5613–5624. D. D. S. Fung, L. F. Qiao, W. C. H. Choy, C. D. Wang, W. E. I Sha, F. X. Xie and S. L. He J. Mater. Chem. 2011, 21, 16349-56
- [27] Negishi, Y.; Nobusada, K.; Tsukuda, T. Glutathione-Protected Gold Clusters Revisited: Bridging the Gap between gold(I)-Thiolate Complexes and Thiolate-Protected Gold Nanocrystals J. Am. Chem. Soc. 2005, 127, 5261– 5270 [ACS Full Text ACS Full Text], [PubMed], [CAS]
- [28] Zheng, J.; Zhang, C.; Dickson, R. Highly Fluorescent, Water-Soluble, Size-Tunable Gold Quantum Dots Phys. Rev. Lett. 2004, 93, 077402 [CrossRef], [CAS]
- [29] Negishi, Y.; Sakamoto, C.; Ohya, T.; Tsukuda, T. Synthesis and the Origin of the Stability of Thiolate-Protected Au 130 and Au 187 Clusters J. Phys. Chem. Lett. 2012, 3, 1624– 1628 [ACS Full Text ACS Full Text], [CAS]
- [30] Yu, Y.; Chen, X.; Yao, Q.; Yu, Y.; Yan, N.; Xie, J. Scalable and Precise Synthesis of Thiolated Au 10–12, Au 15, Au 18, and Au 25 Nanoclusters via pH Controlled CO Reduction Chem. Mater. 2013, 25, 946– 952 [ACS Full Text ACS Full Text], [CAS]
- [31] Stamplecoskie, K. G.; Kamat, P. V. Size-Dependent Excited State Behavior of Glutathione-Capped Gold Clusters and Their Light-Harvesting Capacity J. Am. Chem. Soc. 2014, 136, 11093– 11099 [ACS Full Text ACS Full Text], [PubMed], [CAS]
- [32] Wu, Z.; Jin, R. On the Ligand's Role in the Fluorescence of Gold Nanoclusters Nano Lett. 2010, 10, 2568– 2573 [ACS Full Text ACS Full Text], [PubMed], [CAS]
- [33] Azcarate, J. C.; Corthey, G.; Pensa, E.; Vericat, C.; Fonticelli, M. H.; Salvarezza, R. C.; Carro, P. Understanding the Surface Chemistry of Thiolate-Protected Metallic Nanoparticles J. Phys. Chem. Lett. 2013, 4, 3127– 3138 [ACS Full Text ACS Full Text], [CAS]
- [34] Chen, W.-T.; Hsu, Y.-J.; Kamat, P. V. Realizing Visible Photoactivity of Metal Nanoparticles: Excited-State Behavior and Electron-Transfer Properties of Silver (Ag 8) Clusters J. Phys. Chem. Lett. 2012, 3, 2493– 2499 [ACS Full Text ACS Full Text], [CAS]
- [35] Negishi, Y.; Iwai, T.; Ide, M. Continuous Modulation of Electronic Structure of Stable Thiolate-Protected Au25 Cluster by Ag Doping Chem. Commun. 2010, 46, 4713– 4715 [CrossRef], [PubMed], [CAS]
- [36] Fields-Zinna, C. A.; Crowe, M. C.; Dass, A.; Weaver, J. E. F.; Murray, R. W. Mass Spectrometry of Small Bimetal Monolayer-Protected Clusters Langmuir 2009, 25, 7704– 7710 [ACS Full Text ACS Full Text], [PubMed], [CAS]
- [37] Kurashige, W.; Niihori, Y.; Sharma, S.; Negishi, Y. Recent Progress in the Functionalization Methods of Thiolate-Protected Gold Clusters J. Phys. Chem. Lett. 2014, 4134– 4142 [ACS Full Text ACS Full Text], [CAS]